

- (5) J. P. Jarry and L. Monnerie, *J. Polym. Sci., Polym. Phys. Ed.*, **16**, 443 (1978).
- (6) J. P. Jarry, C. Pambrun, P. Sergot, and L. Monnerie, *J. Phys. E*, **11**, 702 (1978).
- (7) J. P. Jarry and L. Monnerie, 16th IUPAC Congress, Tokyo, 1977.
- (8) E. A. Di Marzio, *J. Chem. Phys.*, **36**, 1568 (1962).
- (9) J. L. Jackson, M. C. Shen, and D. A. McQuarrie, *J. Chem. Phys.*, **44**, 2388 (1966).
- (10) T. Tanaka and G. Allen, *Macromolecules*, **10**, 426 (1977).
- (11) P. G. de Gennes, *C. R. Hebd. Seances Acad. Sci., Ser. B*, **281**, 101 (1975).
- (12) W. Maier and A. Saupe, *Z. Naturforsch., A*, **14**, 882 (1959).
- (13) R. M. Humphries, P. G. James, and G. R. Luckhurst, *Symp. Faraday Soc.*, **5**, 107 (1971).
- (14) P. G. de Gennes, "The Physics of Liquid Crystals", Clarendon Press, 1974.
- (15) M. V. Volkenstein, "High Polymers", Vol. 17, Interscience, New York, 1963, Chapter 8.
- (16) H. M. James and E. Guth, *J. Chem. Phys.*, **11**, 455 (1943).
- (17) M. Abramowitz and J. A. Stegun, "Handbook of Mathematical Functions", Dover Publications, New York, 1965.

Wormlike Chains Near the Rod Limit: Translational Friction Coefficient

Takashi Norisuye,* Masanori Motowoka, and Hiroshi Fujita

Department of Polymer Science, Osaka University, Toyonaka, Osaka, 560 Japan.

Received October 13, 1978

ABSTRACT: The translational friction coefficient, Ξ , of the Kratky-Porod (KP) wormlike chain near the rod limit is calculated according to the Yamakawa-Fujii formulation of the Oseen-Burgers method, with a wormlike sausage model assumed for the chain. Here wormlike sausage means a wormlike cylinder capped with hemispheres at its ends. The resulting expression for Ξ converges to the Stokes law at the limit of $L = d$, where L is the contour length and d is the diameter of the sausage. Its comparison with the Yamakawa-Fujii expression, which ignores end effects, shows that end corrections to Ξ are unexpectedly small. In fact, the Yamakawa-Fujii theory is accurate down to as short a chain as $L/d \sim 4$.

Among others,¹⁻⁵ the most accurate formulation of the translational friction coefficient, Ξ , of the Kratky-Porod wormlike chain⁶ (KP chain) is one worked out by Yamakawa and Fujii⁵ with a model that they call the wormlike cylinder. However, it is still incomplete in that it neglects contributions from the ends of the cylinder. Judging from a study by Broersma⁷ on straight cylinders, one may anticipate that end effects on hydrodynamic behavior should become significant as the KP chain gets shorter. The purpose of the present paper is to estimate such effects on Ξ , using a wormlike sausage model for the KP chain. This model is a wormlike cylinder capped with two hemispheres at its ends, as illustrated in Figure 1. It is assumed that the central axis of the sausage has a flexibility characteristic of the KP chain. We also assume that the cross-section of each hemisphere perpendicular to the central axis stays circular in whatever way the sausage is deformed. Our calculation will be restricted to the sausage near the rod limit, because by so doing the previously derived moments⁵ $\langle \mathbf{R}^{2m}(\mathbf{R} \cdot \mathbf{u}_0)^n \rangle$ ($m, n = 0, 1, 2, \dots$) for the KP chain can be applied to calculate the mean reciprocal distance $\langle |\mathbf{R} - \mathbf{r}|^{-1} \rangle$, which is basic to the evaluation of Ξ by the Yamakawa-Fujii formula.⁵ Various symbols appearing here will be explained in the text.

Mean Reciprocal Distance

As in the Yamakawa-Fujii formulation, we measure all lengths in units of the Kuhn statistical length $2q$, where q is the persistence length of a given KP chain.

Consider two points x and y on the central axis or contour of a wormlike sausage and place the origin of Cartesian coordinates (X, Y, Z) at the point x (see Figure 1). Let the spherical coordinates of \mathbf{R} and \mathbf{u}_0 be denoted by $\mathbf{R} = (R, \Theta, \Phi)$ and $\mathbf{u}_0 = (1, \theta_0, \phi_0)$, respectively. Here, as shown in Figure 1, \mathbf{R} is the distance between the points x and y , and \mathbf{u}_0 is the unit vector for the tangent to the contour at the point x . An orthogonal curvilinear coordinate system (ξ, η, ζ) may be defined in such a way that

the ξ, η , and ζ axes are in the directions of \mathbf{e}_{u_0} , \mathbf{e}_{θ_0} , and \mathbf{e}_{ϕ_0} , respectively, where \mathbf{e} denotes a unit vector. Let the components of \mathbf{R} in this coordinate system be denoted by R_ξ, R_η , and R_ζ :

$$\mathbf{R} = (R_\xi, R_\eta, R_\zeta) \quad (1)$$

It is a simple operation to show that

$$R_\xi = R[\cos \theta_0 \cos \Theta + \sin \theta_0 \sin \Theta \cos (\Phi - \phi_0)]$$

$$R_\eta = R[-\sin \theta_0 \cos \Theta + \cos \theta_0 \sin \Theta \cos (\Phi - \phi_0)]$$

$$R_\zeta = R \sin \Theta \sin (\Phi - \phi_0) \quad (2)$$

where $R = |\mathbf{R}|$. Let \mathbf{r} be the radius vector at the point x . If the angle that it makes with the η axis is denoted by β , the ξ, η , and ζ components of \mathbf{r} are given by

$$\mathbf{r} = (0, r \cos \beta, r \sin \beta) \quad (3)$$

Equations 1 and 3 may allow $|\mathbf{R} - \mathbf{r}|^{-1}$ to be written in the form

$$|\mathbf{R} - \mathbf{r}|^{-1} = 1/[R^2 + r^2 - 2r(R_\eta \cos \beta + R_\zeta \sin \beta)]^{1/2} \quad (4)$$

The mean reciprocal distance $\langle |\mathbf{R} - \mathbf{r}|^{-1} \rangle$ is given by⁵

$$\langle |\mathbf{R} - \mathbf{r}|^{-1} \rangle = \int \langle |\mathbf{R} - \mathbf{r}|^{-1} \rangle_\beta G(\mathbf{R}, \mathbf{u}_0; t) d\mathbf{R} d\mathbf{u}_0 \quad (5)$$

where $G(\mathbf{R}, \mathbf{u}_0; t)$ is a distribution function ($t = |x - y|$) and

$$\langle |\mathbf{R} - \mathbf{r}|^{-1} \rangle_\beta = \frac{1}{2\pi} \int_0^{2\pi} |\mathbf{R} - \mathbf{r}|^{-1} d\beta \quad (6)$$

The integral in eq 6 with eq 4 can be evaluated to give

$$\langle |\mathbf{R} - \mathbf{r}|^{-1} \rangle_\beta = \frac{1}{(R^2 + r^2)^{1/2}} \sum_{m=0}^{\infty} \frac{(4m-1)!!}{4^m(m!)^2} \left(\frac{Rr \sin \theta}{R^2 + r^2} \right)^{2m} \quad (7)$$

where θ is the angle between the vectors \mathbf{R} and \mathbf{u}_0 , and $(4m$

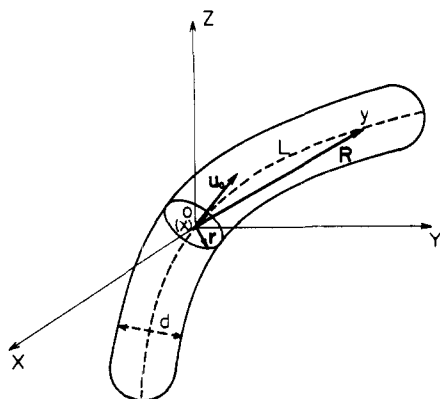


Figure 1. Wormlike sausage model and coordinate system taken for the calculation of the mean reciprocal distance $\langle |\mathbf{R} - \mathbf{r}|^{-1} \rangle$.

$-1)!! = (4m-1)(4m-5)\dots 7\cdot 3\cdot 1$. Introduction of eq 7 into eq 5, followed by integration, and use of $R \cos \theta = \mathbf{R} \cdot \mathbf{u}_0$ yield

$$\langle |\mathbf{R} - \mathbf{r}|^{-1} \rangle = \sum_{m=0}^{\infty} \sum_{j=0}^{\infty} \sum_{n=0}^m \frac{(-1)^{n+j} (4m-1)!! \Gamma(j+2m+\frac{1}{2})}{4^m m! n! (m-n)! \Gamma(2m+\frac{1}{2}) \Gamma(j+1)} \times r^{2m+2j} \langle R^{-2m-2n-2j-1} (\mathbf{R} \cdot \mathbf{u}_0)^{2n} \rangle \quad (8)$$

where Γ denotes the gamma function. The moments $\langle R^{-2m-2n-2j-1} (\mathbf{R} \cdot \mathbf{u}_0)^{2n} \rangle$ remain finite near the rod limit, because they approach $t^{-2m-2j-1}$ at this limit. They can be obtained from the previously derived expression⁸ for $\langle R^{2l} (\mathbf{R} \cdot \mathbf{u}_0)^{2n} \rangle$ simply by putting $l = -m-n-j-1/2$. If the result obtained is introduced into eq 8 and the sums are evaluated, then we obtain

$$\langle |\mathbf{R} - \mathbf{r}|^{-1} \rangle \equiv K(x, y) = \frac{1}{t(1+h)^{1/2}} (1 + f_1 t + f_2 t^2 + f_3 t^3 + f_4 t^4 + f_5 t^5 + \dots) \quad (9)$$

Here

$$f_1 = (1 + 4h)/3(1 + h)^2$$

$$f_2 = (2 + 9h + 117h^2 - 65h^3)/30(1 + h)^4$$

$$f_3 = (8 + 27h - 1437h^2 + 19337h^3 - 17952h^4 + 1680h^5)/630(1 + h)^6$$

$$f_4 = \frac{1}{2520(1 + h)^8} (8 + 24h - 119h^2 - 158350h^3 + 1041375h^4 - 1163234h^5 + 258025h^6 - 6776h^7)$$

$$f_5 = \frac{1}{27720(1 + h)^{10}} (32 + 108h + 4725h^2 + 1090642h^3 - 43431969h^4 + 213481842h^5 - 264917359h^6 + 91970484h^7 - 7445064h^8 + 64064h^9) \quad (10)$$

$$t = |x - y| \quad (11)$$

$$h = r^2/t^2 \quad (12)$$

and

$$r = (dx - x^2)^{1/2} \quad \text{for } 0 \leq x < d/2$$

$$r = d/2 \quad \text{for } d/2 \leq x \leq L - d/2 \quad (13)$$

$$r = [d(L - x) - (L - x)^2]^{1/2} \quad \text{for } L - d/2 < x \leq L$$

with d and L being respectively the reduced diameter and the reduced contour length of the sausage. Note that for the wormlike cylinder model by Yamakawa and Fujii⁵ r

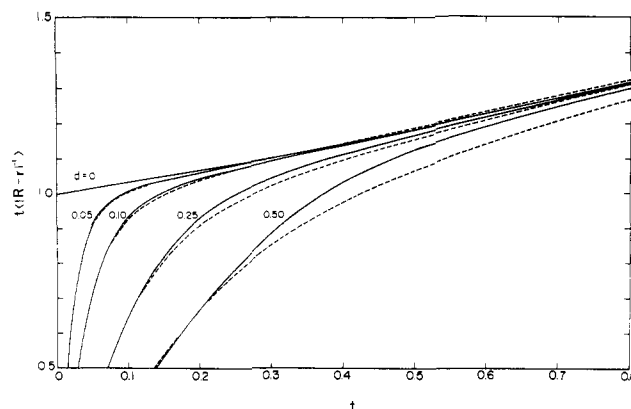


Figure 2. Values of $t \langle |\mathbf{R} - \mathbf{r}|^{-1} \rangle$ calculated from eq 9 with $h = (d/2t)^2$ for the indicated values of d . The dashed lines indicate the Yamakawa-Fujii approximation.⁵

is equal to $d/2$ for all x , $0 < x < L$. If r is taken to be zero, eq 9 reduces to

$$\langle 1/R \rangle = \frac{1}{t} \left(1 + \frac{t}{3} + \frac{t^2}{15} + \frac{4t^3}{315} + \frac{t^4}{315} + \frac{4t^5}{3465} + \dots \right) \quad (14)$$

which agrees with our previous expression⁸ derived from the distribution function $G(\mathbf{R}; t)$.

Figure 2 shows the curves of $t \langle |\mathbf{R} - \mathbf{r}|^{-1} \rangle$ vs. t calculated from eq 9 with $h = (d/2t)^2$ for the indicated values of d . For comparison, the Yamakawa-Fujii values⁵ obtained by the cubic approximation of Hearst and Stockmayer² are shown by the dashed lines. The Yamakawa-Fujii values come close to ours, particularly for small d and at small t values. We note, however, that although our f_i in eq 9 are functions of both d and t , the corresponding coefficients for t^i ($i = 1, 2, 3$) in the Yamakawa-Fujii approximation depend only on d .

Translational Friction Coefficient

According to the Oseen-Burgers procedure^{9,10} developed by Yamakawa and Fujii,⁵ the reduced translational friction coefficient Ξ of a continuous chain of reduced contour length L can be calculated from

$$\Xi = 6\pi\eta_0 L^2 \left[\int_0^L \int_0^L K(x, y) dx dy \right]^{-1} \quad (15)$$

where η_0 denotes the viscosity of the solvent. Before proceeding to the calculation of Ξ of a wormlike sausage, we examine the accuracy of eq 15 by calculating Ξ of some rigid particles for which exact values are known.

Rigid Rods and Spheres

In the rod limit, where both t and d approach zero, eq 9 reduces to

$$K_0(x, y) = 1/[(x - y)^2 + r^2]^{1/2} \quad (16)$$

where the subscript 0 refers to the rod limit. Introduction of this equation with eq 13 into eq 15, followed by integration, yields

$$\frac{3\pi\eta_0 L}{\Xi_0} = \ln \frac{2L - d + (4L^2 - 4Ld + 2d^2)^{1/2}}{d} + \frac{L + (2^{1/2}d) - (4L^2 - 4Ld + 2d^2)^{1/2}}{L} + (d/2L) \ln \frac{(2^{1/2} - 1)^2 [d + (4L^2 - 4Ld + 2d^2)^{1/2}]}{2L - d + (4L^2 - 4Ld + 2d^2)^{1/2}} \quad (17)$$

When $L \gg d$, this approaches

$$3\pi\eta_0 L/\Xi_0 = \ln(L/d) + 2 \ln 2 = 1 + 0(d/L) \quad (18)$$

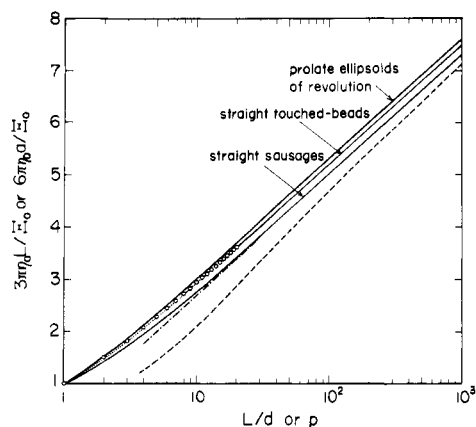


Figure 3. Translational friction coefficients of the indicated rigid particles. Dashed line: Broersma's theory⁷ for rigid cylinders. Dot-Dash line: asymptotic values for straight sausages.

which conforms to the Yamakawa-Fujii asymptotic expression⁵ for long rigid cylinders. On the other hand, in the limit of $L = d$, eq 17 reduces to

$$\Xi_0 = 6\pi\eta_0(d/2) \quad (19)$$

which is the well-known Stokes equation. These limiting properties of eq 17 are consistent with the geometric features of our wormlike sausage.

Ellipsoids of Revolution

If eq 15 is applied to a prolate ellipsoid of revolution for which r^2 in eq 16 is given by $b^2 - (b/a)^2(x - a)^2$, we obtain

$$\Xi_0 = \frac{6\pi\eta_0 a(p^2 - 1)^{1/2}}{p \ln [p + (p^2 - 1)^{1/2}]} \quad (20)$$

where a and b are respectively the semimajor and semiminor axes of the ellipsoid and p is the axial ratio defined by

$$p = a/b \quad (21)$$

Equation 20 happens to agree with the Perrin equation¹¹ for rigid prolate ellipsoids of revolution. The Perrin equation for rigid oblate ellipsoids of revolution can also be derived in a similar way.

Figure 3 shows values of $3\pi\eta_0 L/\Xi_0$ for straight sausages and $6\pi\eta_0 a/\Xi_0$ for prolate ellipsoids of revolution. For comparison, the $3\pi\eta_0 L/\Xi_0$ values calculated from eq A-2 (in the Appendix) for straight rods composed of touched-spherical beads are also shown. These values all start with the Stokes value and follow slightly different curves. Since eq 17, 20, and A-2 have been derived on the same approximation (see the Appendix), the small differences may be ascribed to the geometric differences of the models. The dashed line in Figure 3 indicates Broersma's values⁷ of $3\pi\eta_0 L/\Xi_0$ for rigid cylinders with the end corrections taken up to terms of $(d/L)^2$. Its discrepancy from the other curves is quite large. The asymptotic expression of Broersma for rigid cylinders is essentially the same as eq 18. Thus the large discrepancy of Broersma's values from ours for straight sausages ought to have its root in the terms of the first and higher orders in d/L . We here remark that the shell-model values of $3\pi\eta_0 L/\Xi_0$ calculated by Bloomfield et al.¹² for rigid cylinders agree quite closely with our values for straight sausages over the entire range of L/d and that the analysis by Record et al.¹³ of sedimentation coefficient data for short DNA in terms of the Broersma theory led to an unreasonably large diameter (about 5 nm) for DNA molecules.

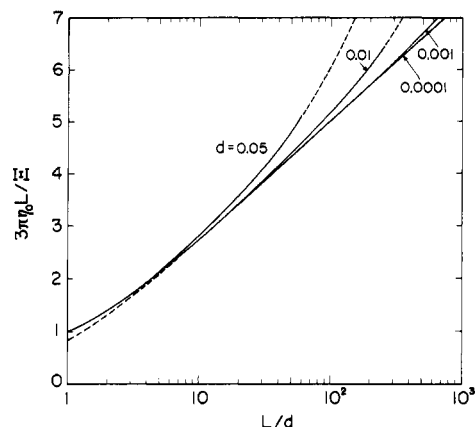


Figure 4. Values of $3\pi\eta_0 L/\Xi$ for wormlike sausages calculated from eq 22 for the indicated values of d . The dashed lines indicate the Yamakawa-Fujii theory⁵ for wormlike cylinders.

Wormlike Chains

For the KP chain we may substitute eq 9 into eq 15. The final expression then obtained for Ξ is so lengthy that we here show its form expanded in powers of d/L . It reads

$$3\pi\eta_0 L/\Xi = C_1 \ln(L/d) + C_2 + C_3 L + C_4 L^2 + C_5 L^3 + C_6 L^4 + C_7 L^5 + \dots \quad (22)$$

where

$$C_1 = 1 - 0.1250(d/L)d + 0.1406(d/L)d^3 + \dots$$

$$C_2 = 0.3863 + 0.6863(d/L) - 0.06250(d/L)^2 - 0.01042(d/L)^3 - 0.0006510(d/L)^4 + 0.0005859(d/L)^5 + \dots$$

$$C_3 = 0.1667 - 0.06838(d/L)^2 + 0.02083(d/L)^3 - 0.01693(d/L)^4 - 0.008594(d/L)^5 + \dots$$

$$C_4 = 0.01111 + 0.07917(d/L)^2 - 0.1799(d/L)^3 + 0.1055(d/L)^4 + 0.02461(d/L)^5 + \dots$$

$$C_5 = 0.001058 - 0.004960(d/L)^2 + 0.001653(d/L)^3 - 0.07348(d/L)^4 - 0.03281(d/L)^5 + \dots$$

$$C_6 = 0.0001587 - 0.0007275(d/L)^2 + 0.0003638(d/L)^3 - 0.08630(d/L)^4 + 0.4000(d/L)^5 + \dots$$

$$C_7 = 0.00003848 - 0.0001714(d/L)^2 + 0.0001142(d/L)^3 + 0.006183(d/L)^4 - 0.002897(d/L)^5 + \dots \quad (23)$$

If both L and d are allowed to approach zero, keeping $L/d = 1$, eq 22 approaches $3\pi\eta_0 d/\Xi = 0.9996$, which is substantially identical with eq 19, the Stokes relation for rigid spheres.

In Figure 4, the values of $3\pi\eta_0 L/\Xi$ calculated from eq 22 are plotted against L/d for a series of d values, together with those predicted by the Yamakawa-Fujii theory⁵ (dashed lines). Except for fairly small L/d , both theories give essentially the same results. Our larger values in the region of small L/d can be ascribed to the hemispherical end caps. Mathematically, such end effects appear as terms of the first and higher orders of d/L in eq 23. They are rather small even for L/d not sufficiently removed from unity: less than 3% for $L/d \geq 4$ and about 18% for $L/d \sim 1$. Thus, if $L/d \geq 4$, contributions from the hemispherical ends have a minor effect on the translational friction coefficient of the KP chain. Record et al.¹³ have found a good agreement between their sedimentation coefficient data on DNA and the Yamakawa-Fujii theory

down to $L/d \sim 10$. The present work theoretically substantiates their finding and suggests even a wider range of applicability (down to $L/d \sim 4$) of the Yamakawa–Fujii formula for Ξ of the wormlike cylinder.

Appendix

We wish to calculate Ξ_0 for the straight touched beads model, using the same Oseen–Burgers procedure as for continuous models. The equation derived by Fujita (eq 7 in ref 14) for the beads model is pertinent to this purpose. When the Kirkwood–Riseman approximation¹⁵ is used, it gives

$$3\pi\eta_0 nd/\Xi_0 = 1 + (d/2n) \sum_{i \neq j} \langle 1/R_{ij} \rangle \quad (\text{A1})$$

for a straight rod composed of n touched spherical beads of diameter d . Here $\langle 1/R_{ij} \rangle$ is the mean reciprocal distance between the i th and the j th beads. Introduction of the relation $\langle 1/R_{ij} \rangle = (|j - i|d)^{-1}$ into eq A-1, followed by summation, gives

$$3\pi\eta_0 nd/\Xi_0 = \psi(n+1) + \gamma \quad (\text{A2})$$

where γ is the Euler constant equal to 0.5772 and ψ is defined by

$$\psi(z) = \frac{d}{dz} \ln \Gamma(z)$$

Since $\psi(n+1) = \ln n + 1/(2n) - 1/(12n^2) + 1/(120n^4) + \dots$ for $n \gg 1$, replacement of nd by L yields

$$3\pi\eta_0 L/\Xi_0 = \ln(L/d) + 0.5772 + (1/2)(d/L) - (1/12)(d/L)^2 + (1/120)(d/L)^4 + \dots \quad (\text{A3})$$

References and Notes

- (1) O. B. Ptitsyn and Yu. E. Eizner, *Vysokomol. Soedin.*, **3**, 1863 (1961).
- (2) J. E. Hearst and W. H. Stockmayer, *J. Chem. Phys.*, **37**, 1425 (1962).
- (3) A. Peterlin, *J. Polym. Sci.*, **8**, 173 (1952).
- (4) R. Ullman, *J. Chem. Phys.*, **53**, 1734 (1970).
- (5) H. Yamakawa and M. Fujii, *Macromolecules*, **6**, 407 (1973).
- (6) O. Kratky and G. Porod, *Recl. Trav. Chim. Pays-Bas*, **68**, 1106 (1949).
- (7) S. Broersma, *J. Chem. Phys.*, **32**, 1632 (1960).
- (8) T. Norisuye, H. Murakami, and H. Fujita, *Macromolecules*, **11**, 966 (1978).
- (9) C. W. Oseen, "Hydrodynamik", Akademische Verlagsgesellschaft, Leipzig, 1927.
- (10) J. M. Burgers, "Second Report on Viscosity and Plasticity of the Amsterdam Academy of Sciences", Nordemann, New York, 1938, Chapter 3.
- (11) F. Perrin, *J. Phys. Radium*, **7**, 1 (1936).
- (12) V. A. Bloomfield, K. E. Van Holde, and W. O. Dalton, *Biopolymers*, **5**, 149 (1967).
- (13) M. T. Record, Jr., C. B. Woodbury, and R. B. Inman, *Biopolymers*, **14**, 393 (1975).
- (14) H. Fujita, *J. Polym. Sci., Polym. Phys. Ed.*, **11**, 899 (1973).
- (15) J. G. Kirkwood and J. Riseman, *J. Chem. Phys.*, **16**, 565 (1948).

Surface Studies on Multicomponent Polymer Systems by X-ray Photoelectron Spectroscopy. Polystyrene/Poly(ethylene oxide) Diblock Copolymers

H. Ronald Thomas* and James J. O'Malley

Xerox Corporation, Webster Research Center, Rochester, New York 14644.
Received July 13, 1978

ABSTRACT: X-ray photoelectron spectroscopy (XPS) is a surface characterization technique capable of providing detailed information about the structure and bonding of molecules in the solid state. In this study, we have used XPS to elucidate the surface topography and copolymer composition of a series of polystyrene/poly(ethylene oxide) diblock copolymer thin films at the polymer–air interface. These copolymers undergo microphase separation when solvent cast into films. The XPS results clearly indicate that the copolymer compositions of the surfaces (e.g., outermost ~ 50 Å) are significantly different from the overall bulk compositions. Surface excesses of polystyrene are observed in all copolymer films cast from chloroform, ethylbenzene, and nitromethane. Angular dependent XPS studies [XPS(θ)] support a model for the topography of the copolymer surfaces that has isolated domains of each homopolymer at the surface appearing thick on the XPS scale of ~ 50 Å with a fractional area coverage proportional to the mole percent bulk composition of the copolymers.

The application of X-ray photoelectron spectroscopy (XPS) to the study of polymer surfaces has been pioneered by Clark and co-workers over the past few years.^{1–3} The inherent surface sensitivity (top few tens of angstroms) of XPS enables one to differentiate the surface from the subsurface structure and bonding in particular systems. Simply, the XPS experiment involves the measurement of binding energies of electrons ejected by interactions of a molecule with a monoenergetic beam of soft X-rays.⁴ The surface sensitivity and the capability of differentiating the surface from subsurface are a consequence of the extremely short (<100 Å) mean free paths (λ) of electrons and their strong dependence on kinetic energy.⁵ By taking advantage of (1) the differences in λ associated with electrons from different core levels in the same or different atoms and (2) angular XPS studies [XPS(θ)],³ it is possible to depth profile the compositional variations in the surfaces of solids.

In this work we have utilized XPS to investigate the influence of chemical composition and film casting solvent on the surface structure of polystyrene (PS)–poly(ethylene oxide) (PEO) diblock copolymers. Earlier studies^{6,7} of the bulk morphologies and properties of the copolymers indicated that the PS and PEO components are highly incompatible and that they readily undergo microphase separation and domain formation. These studies also showed that the bulk morphology of the copolymer films was profoundly influenced by the solvent from which the films were cast. On the other hand, there have been no investigations of the surface properties of these copolymers and, in particular, their surface composition and topography at the air–copolymer interface. We can anticipate, however, that the surface and the bulk will not be identical because of the significant differences in the solid state surface tension of PS (36 dyn/cm)⁸ and PEO (44 dyn/cm).⁸ The XPS studies have indeed revealed significant dif-